Extension dynamics of discotic nematics of variable order : geodesic flow and viscoelastic relaxation

Arvinder Singh, Alejandro Rey

Classification
Physics Abstracts
46.20 — 46.60B — 61.30

Extension dynamics of discotic nematics of variable order : geodesic flow and viscoelastic relaxation

Arvinder P. Singh and Alejandro D. Rey

Department of Chemical Engineering, McGill University, Montreal, Quebec, Canada H3A 2A7

(Received 2 September 1993, received in final form 16 November 1993, accepted 10 January 1994)

Abstract. — Variational methods are used to develop the governing equations that describe the flow of spatially invariant uniaxial discotic nematic liquid crystals of variable order ; since the equations are based on a phenomenological truncated expansion of the entropy production, the equations are approximations. Restrictions in the phenomenological parameters appearing in the governing equations are imposed taking into account the ordering of the discotic phase. Numerical and analytical solutions of the director **n** and alignment S are presented for a given uniaxial extensional start-up flow. The unit sphere description of the director is used to discuss and analyze the sensitivity of the director trajectories and the coupled alignment relaxation to the initial conditions ($\mathbf{n}_0$, S_0) and to the alignment Deborah number (De). The numerical results are used to characterize the relaxation of the tensor order parameter **Q** and to compute the steady flow birefringence. When the poles of the unit sphere are along the extension axis and the equator lies in the compression plane of the flow, it is found that the director trajectories belong to the meridians (great circles through the poles) and the dynamics follows a geodesic flow ; when subjected to flow the director follows the shortest path that connects the initial orientation $\mathbf{n}_0$ and the equator (compression plane). As typical of geodesic flows, there is a strong sensitivity to initial conditions : when $\mathbf{n}_0$ lies on the poles no predictions on the eventually steady director orientation are possible. If the prior to flow orientation is close to the poles the coupled alignment relaxation along the geodesics is nonmonotonic and for large De the discotic may become temporarily isotropic. The couplings between **n** and S are captured by the tensor order parameter relaxation. At steady state, the director lies on the equator, and the alignment and birefringence increase with increasing De.

1. Introduction.

Discotic nematic liquid crystals are an important class of mesophases that occur naturally in carbonaceous mesophases [1-3]. These mesophases are formed by condensation of aromatic rings and tend to adopt a uniaxial discotic nematic phase Nd [4, 5], with the unit normals to the disc-like molecules more or less aligned along a common direction (see Fig. 1b), represented by the director **n** ; in what follows we use **n** and orientation interchangeably. These materials find practical use in the spinning of high performance carbon fibers [2, 3, 6], and

understanding their flow orienting behavior in the presence of uniaxial extensional deformations is of practical utility. As a first step in developing a basic qualitative understanding of such complex nonlinear problem, in this work we consider the flow orienting properties of a model incompressible discotic nematic liquid crystal of variable degree of order in isothermal uniaxial extensional flow.

Previous work [7-11] on the rheology and flow-induced orientation of uniaxial discotic nematics assumed that the scalar order parameter S remains unaffected by the flow ; in what follows we use S and alignment interchangeably. The validity of this assumption for low molar mass materials justifies then the use of the Leslie-Ericksen (L-E) theory [12, 13] for uniaxial nematics with the proper values of the material parameters. The important differences in sign and magnitude of the material parameters corresponding to uniaxial rod-like and discotic nematics follow from the fact that rod-like nematics orient their longest molecular dimension along the director while disc-like nematics orient their shortest molecular dimension along the director. As is well-known, the orienting properties of uniaxial nematics during shear flow are governed by the sign and magnitude of the tumbling (reactive) parameter λ : for aligning (non-aligning) rods $\lambda > 1$ $(0 < \lambda < 1)$, and for aligning (non-aligning) discs $\lambda < -1 (-1 < \lambda < 0)$; the tumbling parameter λ is given by the negative ratio of the irrotational torque coefficient (γ_2) and the rotational viscosities (γ_1), and represents the coefficient of the ratio of strain to vorticity torques acting on the director **n**. Previous work [8, 9] focused on the orienting properties of aligning uniaxial discotic nematics in steady shear, and it was found that shear orients the director in the shear plane and at a steady angle θ, lying in the $90° \leq \theta \leq 135°$ sector with respect to the flow direction. In steady shear-free uniaxial extensional flows, the orienting behavior of uniaxial nematics is again determined by the sign of λ : when $\lambda > 0$ the director aligns along the stretching (extension) direction, and when $\lambda < 0$ the director aligns somewhere in the compression plane, orthogonal to the stretching direction [11].

For materials of larger molecular weights the coupling between the director and the scalar order parameter should be retained [14]. This coupling introduces additional nonlinearities through the dependence of the generalized Leslie coefficients on the scalar order parameter, as shown in various works [14-18]. The nonlinear shear orienting behavior of rod- and disk-like nematics is now dependent on the shear rate, and flow-induced transitions involving aligning and non-aligning modes are triggered by varying the shear rate [18-20]. On the other hand, the behavior of rod-like nematics in extension is less dramatic since the competition between shear and vorticity is absent in an irrotational flow, and the effect of flow is to orient the director along the stretching direction with a concomitant increase in the scalar order parameter. A more complex situation presents itself for the uniaxial extension of discotic nematics, since they may orient anywhere in the compressional orthogonal plane, and may exhibit a nonlinear relaxation of S. The former observation explains the various observed cross section morphologies of mesophase carbon fibers, in which the normals to the molecular planes lies in the plane normal to the fiber axis [6, 21].

Our main objective in this work is to establish the relevant qualitative features that describe the relations between uniaxial extensional deformation inputs and orientation and alignment responses in an idealized discotic nematic liquid crystal. In the present paper the phenomenological properties of the particular model discotic nematic liquid crystal chosen for study are not fitted to those of any existing real material, and, as shown below, their choice is based on previous results. The particular objectives of this paper are :

(i) to formulate and solve an approximate phenomenological theory that describes the orientation and alignment of a model discotic nematic liquid crystal of variable alignment, during isothermal, incompressible, uniaxial extensional flow ;

(ii) to characterize the sensitivity of the director paths to the compressional plane, to the initial conditions and to the extension rate by using numerical simulation ;

(iii) to characterize the alignment relaxation along the director paths, to the initial conditions and to the extension rate by using numerical simulation ;

(iv) to determine the minimizing principle that governs the director trajectories to the compression plane.

In this paper we use the unit sphere description of nematics [22-25] only to facilitate the discussion and classification of the numerical results that pertain to the above mentioned objectives (ii), (iii) and (iv).

The organization of this paper is as follows. In section 2 we define the coordinate system and the state variables, derive the governing equations, and briefly present the elements of the unit sphere description used to discuss and classify the numerical solutions. A brief description of the numerical method used to integrate the governing equations is presented. In section 3 we present, discuss, and classify the solution vector, consisting of the time dependent director and alignment fields, obtained from numerical integration of the governing equations. Typical computations of the tensor order parameter relaxation and steady flow birefringence are presented.

2. Governing equations.

2.1 DEFINITIONS OF COORDINATES, ORIENTATION AND ALIGNMENT. — In this paper we study the microstructural temporal and spatially invariant response of a model uniaxial discotic nematic subjected at time $t = 0$ to a constant uniaxial extension rate $\dot{\epsilon}$. In what follows we use Cartesian tensor notation, repeated indices are subjected to the summation convention [26], partial differentiation with respect to the jth spatial coordinate is denoted by a comma (i.e. $v_{i,j} = \partial v_i/\partial x_j$) or by the symbol ∂j (i.e. $v_{i,j} = \partial_j v_i$), and a superposed dot denotes the material time derivative (i.e. $\dot{S} = \dfrac{dS}{dt} = \partial S/\partial t + v_i\, \partial_i S$). The microstructure of the nematic is characterized by the uniaxial tensor order parameter $Q_{ij}(t)$ [13] :

$$Q_{ij} = S(n_i\, n_j - \delta_{ij}/3) \tag{1a}$$

where the following restrictions apply :

$$Q_{ij} = Q_{ji} ; \quad Q_{ii} = 0 ; \quad -1/2 \leqslant S \leqslant 1 ; \quad n_i\, n_i = 1 \tag{1b}$$

and δ_{ij} is the unit tensor. The magnitude of the scalar order parameter S is a measure of the molecular alignment along the director $\mathbf{n}$, and is given by $S = 3(n_i\, Q_{ij}\, n_j)/2$. Equation (1a) gives a proper description of the order in a discotic nematic phase if we identify the director as the average orientation of the unit normals to the molecular discs ; see figure 1b ; as explained in [27], with this identification, S is positive for both rod-like and disc-like uniaxial nematic liquid crystals, and no further distinction is required in this paper since rods are not considered here. Since uniaxial extensional flow will not induce negative values for the scalar order parameter S we further restrict its variation to the positive unit interval, $0 \leqslant S \leqslant 1$ [27].

To enforce the unit length constraint $\mathbf{n} \cdot \mathbf{n} = 1$ and to visualize the director orbits on the unit sphere, we parametrize the director with :

$$\mathbf{n} = (n_x, n_y, n_z) = (\cos\phi, \sin\phi \cos\theta, \sin\phi \sin\theta) \tag{2}$$

as shown in figure 1a ; $\theta\,(0 \leqslant \theta \leqslant 2\pi)$ is the azimuthal angle and $\phi\,(0 \leqslant \phi \leqslant \pi)$ is the polar

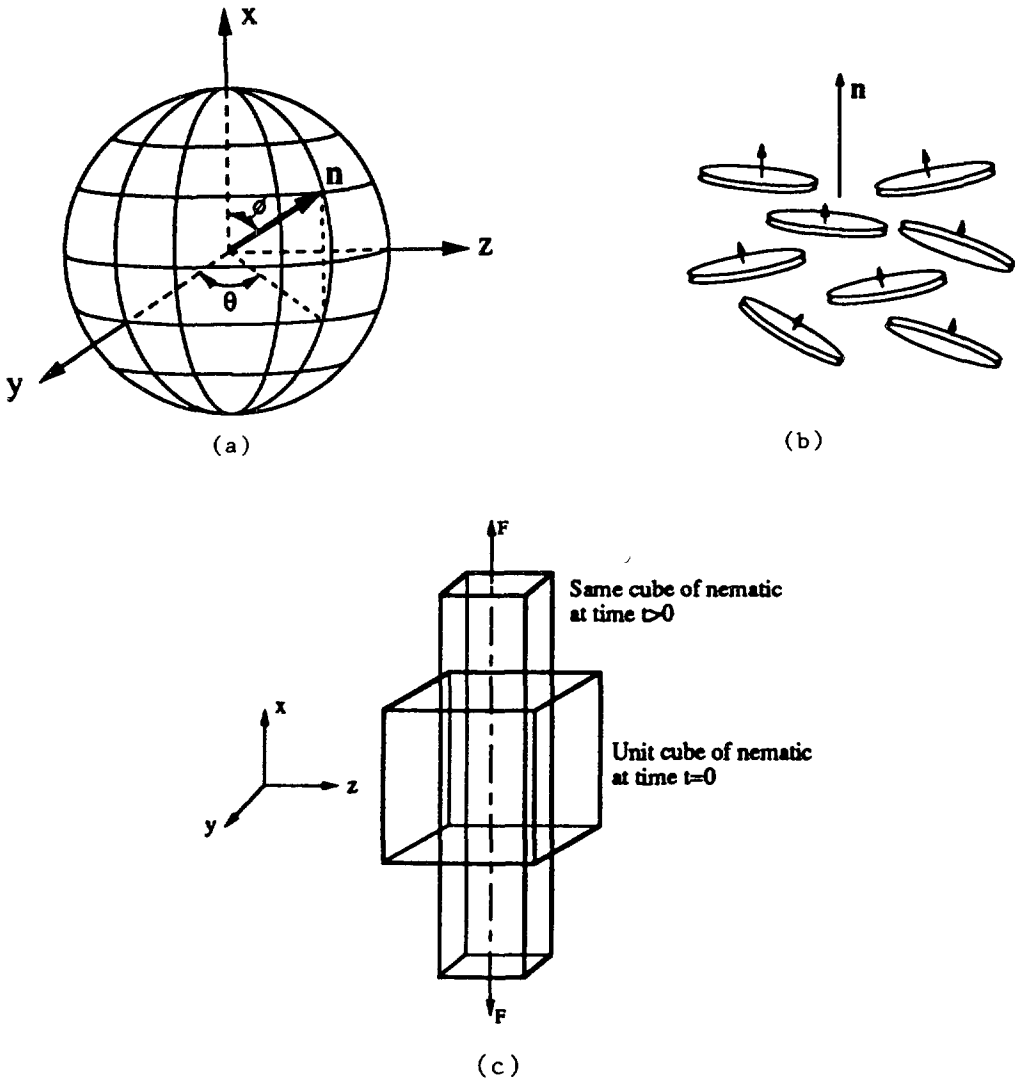

Fig. 1. — Definition of (a) coordinate system, (b) Director orientation of a uniaxial discotic nematic liquid crystal, and (c) uniaxial extensional flow deformation. (a) Director angles and unit sphere : θ ($0 \leq \theta \leq 2\ \pi$) is the azimuthal angle and ϕ ($0 \leq \phi \leq \pi$) is the polar angle. The north pole of the sphere is located at $\phi = 0$, the south pole at $\phi = \pi$, and the equator at (θ, ϕ) = ([0, 2 π], $\pm \pi/2$), **n** denotes the director. (b) The director in a discotic nematic phase is the average orientation of the unit normals to the disc-like molecules. (c) Deformations of a unit cube, submitted to a uniaxial extension deformation along the x-direction.

angle. The north pole of the sphere is located at $\phi = 0$, the south pole at $\phi = \pi$, and the equator at (θ, ϕ) = ([0, 2 π], $\pm \pi/2$).

In the unit sphere description [22-25] the director tip, in the presence of flow, defines a trajectory $O(\mathbf{n}_0)$ on the surface of the sphere :

$$O(\mathbf{n}_0) = \left\{\mathbf{n} \in \Omega^2 \cdot \mathbf{n} = \mathbf{n}(t, \mathbf{n}_0),\ t \in \mathrm{R}^+\right\} \tag{3}$$

where $\mathbf{n}_0 = \mathbf{n}(t = 0)$, Ω^2 denotes the surface of the unit sphere and R^+ the positive reals. To characterize the director orbits $O(\mathbf{n}_0)$ we need to define geodesics and meridians. A geodesic G is the shortest arc connecting two points on the sphere, and is given by [28] :

$$\sin(N_2)\cos\phi - \cos(N_2)\sin\phi\cos\theta - \frac{\sin\phi\sin\theta}{\sqrt{1/N_1^2 - 1}} = 0 \tag{4}$$

where N_1 and N_2 are constants that depend on the two points ; the geodesic or great circle, is the interpection of the sphere with the plane containing the given points and the center of the sphere. When the two points are the poles ($N_2 = \pi$) the degenerate geodesics are the meridians M, which in terms of (θ, ϕ) and the director components (n_i), are given by [28] :

$$\tan\theta = 1/b ; \tag{5a}$$

$$b^2 = 1/(N_1^{-2} - 1) ; \tag{5b}$$

$$0 \leqslant \phi \leqslant \pi ; \tag{5c}$$

$$n_1 = bn_2 ; \tag{6a}$$

$$-1 \leqslant n_1 \leqslant 1 ; \tag{6b}$$

$$-1 \leqslant n_2 \leqslant 1 ; \tag{6c}$$

where $b(-\infty < b < \infty)$ is a constant whose numerical value defines a particular meridian ; a family of meridians is shown in figure 1a.

Figure 1c shows the applied force F and deformations of a cube of discotic nematic subjected at $t = 0$ to a uniaxial extensional flow ; the applied extension and flow direction are along the x-axis (polar axis) and the compression ($y - z$) plane, that contains the equator of the unit sphere, represents the degenerate circle of stable steady director orientation : $\mathbf{n}_{ss} = (0, n_{1ss}, n_{2ss}) = (0, \cos\theta_{ss}, \sin\theta_{ss})$, where the subscript ss denotes steady state.

To characterize the relaxation of the alignment as the director traverses the surface of the sphere, we divide the sphere into three characteristic regions : two equivalent spherical caps on which $|n_1| > 1/\sqrt{3}$, and the remaining spherical zone on which $|n_1| < 1/\sqrt{3}$. In an irrotational uniaxial extensional flow, the only flow effect on the orientation and alignment is due to the symmetric part of the velocity gradient tensor ($v_{i,j}$), usually known as the rate of strain tensor or rate of deformation tensor and denoted by $\mathbf{A}$, and whose ij and ji components are given by $A_{ij} = A_{ji} = (v_{i,j} + v_{j,i})/2$. An important observation, used below to classify the numerical results of alignment relaxation, is that a director whose tip lies in the spherical caps samples extensional strains ($\mathbf{A} : \mathbf{nn} > 0$), while a director whose tip lies in the spherical zone samples compressional strains ($\mathbf{A} : \mathbf{nn} < 0$).

2.2 GOVERNING ORIENTATION AND ALIGNMENT EQUATIONS. — A sufficiently general entropy production density Δ, similar to that proposed by [14], is given by [18] :

$$\begin{aligned} 2D = \Delta = (\nu KT)\,[&\sigma_1(Q_{ij}A_{ji})^2 + \sigma_2(A_{ij}A_{ji}) + \sigma_3(Q_{ij}Q_{ji})A_{\ell k}A_{k\ell} \\ &+ 2\sigma_4(\hat{Q}_{ij}A_{ji}) + 2\sigma_5(Q_{ij}A_{jk}A_{ki}) + 4\sigma_6(\hat{Q}_{ij}Q_{jk}A_{ki}) \\ &+ 2\sigma_7(Q_{ij}Q_{jk}A_{k\ell}A_{\ell i}) + \tau_1(\hat{Q}_{ij}\hat{Q}_{ji}) + 2\tau_2(Q_{ij}\hat{Q}_{jk}\hat{Q}_{ki})] \end{aligned} \tag{7}$$

where the ij components of the corotational time derivative of the tensor order parameter $\hat{\mathbf{Q}}$, and of the vorticity tensor $\mathbf{W}$ are given by :

$$\hat{Q}_{ij} = \frac{\partial Q_{ij}}{\partial t} + v_k Q_{ij,k} - W_{ik}Q_{kj} + Q_{ik}W_{kj} , \tag{8a}$$

$$W_{ij} = (v_{i,j} - v_{j,i})/2 \tag{8b}$$

and where v_k is the k-th component of the linear velocity vector, $\sigma_i (i = 1, \ldots, 7)$ and $\tau_i (i = 1, 2)$ are scalar phenomenological constants with units of time that satisfy certain thermodynamic restrictions such that $\Delta \geq 0$ [14], $1/\nu$ is a molecular volume, T is the absolute temperature, and K is Boltzmann's constant. The most general expansion representing Δ is not closed, but the truncation given by equation (7) is sufficiently general and can be shown to reduce [18] that of Leslie-Ericksen theory [12, 13].

In the absence of spatial gradients ($Q_{ij,k} = 0$) the Lagrangian density Λ is the sum of entropic $\Lambda^{\mathrm{H}}(\mathbf{Q})$ [27] and flow $\Lambda^{\mathrm{F}}(\mathbf{v}, \nabla p, \mathbf{F})$ contributions :

$$\Lambda = \Lambda^{\mathrm{H}} + \Lambda^{\mathrm{F}} \tag{9a}$$

$$\Lambda^{\mathrm{H}} = -\left(\frac{3}{4} A Q_{ij} Q_{ji} + \frac{3}{2} B Q_{mi} Q_{ik} Q_{km} + \frac{9}{16} C (Q_{ik} Q_{ki})^2 \right) \tag{9b}$$

$$\Lambda^{\mathrm{F}} = -u_i (\rho \dot{v}_i + \partial_i p - \rho F_i) \tag{9c}$$

where A, B, and C are temperature dependent phenomenological coefficients, $\mathbf{u}$ is the displacement vector, ρ is the density, p is the pressure, $\mathbf{F}$ is external body force per unit volume. The negative of the entropic contribution Λ^{H} adopted here is known as the excess Landau-de Gennes free energy density [27], which is obtained from a truncated phenomenological expansion in terms of the two independent invariants $Q_{ij} Q_{ji}$ and $Q_{ij} Q_{jk} Q_{ki}$. For uniaxial nematics equation (1a) holds and expression (9b) leads to the following excess free energy density $G(S, T)$ expansion :

$$G = \frac{1}{2} A S^2 + \frac{1}{3} B S^3 + \frac{1}{4} C S^4 \tag{10}$$

Usually, close to the nematic-isotropic transition, B and C are assumed to be independent of temperature, and it is further assumed that $A = a(T - T^*)$, where a is a constant. The cubic term ensures a first order transition at $T_c > T^*$, where T_c is the nematic-isotropic transition temperature and T^* is the temperature at which the free energy has zero curvature at $S = 0$ (@ $S = 0$, $\partial^2 G/\partial S^2 = 0$). For $B < 0$ and for the appropriate temperature range, equation (10) predicts the existence of the normal uniaxial discotic nematic phase, with the molecular unit normals oriented along the director. The minima predicted by equation (10) are :

$$S = 0 \quad \text{(isotropic)} ; \tag{11a}$$

$$S = -\frac{B}{2C} + \sqrt{\left(\frac{B}{2C} \right)^2 - \frac{A}{C}} \quad \text{(nematic)} \tag{11b}$$

Equation (10) predicts the existence of four temperature regions [27] : (i) $T > T^{\#}$: the stable phase is isotropic ; (ii) for $T_c < T < T^{\#}$ · there are two minima, the global one at $S = 0$ (isotropic) and the other one for the superheated nematic phase ; (iii) $T^* < T < T_c$. there are two minima, the global one corresponding to the nematic phase, and the local one corresponding to the supercooled isotropic phase ; (iv) $T < T^*$: there is one minimum corresponding to the nematic phase. At the nematic-isotropic transition temperature $T = T_c$ the free energies of the isotropic and nematic phases are equal and from equation (10) it follows that : (i) $T_c = T^* + 2B^2/(9aC)$, (ii) the value of the order parameter at the transition is $S_c = -2B/(3C)$, and (iii) the latent heat per unit volume for the first order nematic-isotropic transition is $L = 2aB^2 T_c/(9C^2)$. The temperature $T^{\#}$ divides the biphasic region from the single isotropic region and the following holds : (i) $T^{\#} = T^* + B^2/(4aC)$, (ii) $S^{\#} = -B/(2C)$. The temperature T^* is the lowest temperature for which the isotropic phase is

metastable and at that temperature $S^* = -B/C$. Thus a characterization of G requires the specification of the four parameters a, B, C, and T^*. One common way to obtain values for the parameters is to use the Maier-Saupe molecular field theory and express the results in the form of equation (10). Here we use the following adapted results of Doi and Edwards [29], for such parameter mapping between the phenomenological Landau-de-Gennes expansion and the molecular mean field theory :

$$\frac{3}{4}A = \frac{1}{2}\left(1 - \frac{U}{3}\right)\nu KT\,; \tag{12a}$$

$$\frac{3}{2}B = -\frac{U}{3}\nu KT\,; \tag{12b}$$

$$\frac{9}{16}C = \frac{U}{4}\nu KT \tag{12c}$$

where the nematic potential $U = 3\,T^*/T$, and where νKT refer to the same quantities as in equation (7). The two parameters are now ν and U. The resulting excess free energy density now reads :

$$G = \frac{2}{3}\nu KT\left[\frac{1}{2}\left(1 - \frac{U}{3}\right)S^2 - \frac{1}{9}US^3 + \frac{1}{6}US^4\right]. \tag{13}$$

The minima predicted by this free energy are [29] :

$$S = 0 \quad \text{(isotropic)}\,; \tag{14a}$$

$$S = \frac{1}{4} + \frac{3}{4}\sqrt{1 - 8/(3\,U)} \quad \text{(nematic)} \tag{14b}$$

In what follows we use the symbol $S_{eq}(U)$, as given by the right hand side of equation (14b), to denote the equilibrium order parameter in the absence of flow. Comparing (11b) and (14b) it follows that if $B/C = -1/2$, which is generally consistent with nematics [27], both equations predict the same dimensionless temperature dependence of S, as embodied in the term A/C. In addition, equation (13) predicts the existence of four temperature regions with the same thermodynamic behavior as that predicted by equation (10) [29]. In terms of the nematic potential U, the boundaries of these four regions and the values of the alignment S in the nematic phase can be shown to be given by : (i) $U^{\#} = 8/3$, $S^{\#} = 1/4$, (ii) $U_c = 27/10$, $S_c = 1/3$, (iii) $U^* = 3$, $S^* = 1/2$. In this work we use the two parameter equation (13) to construct the Lagrangian Λ^H, since as shown above (see also [29]), it is able to capture with two parameters the same qualitative thermodynamic behavior as the more general equation (10), and because it is consistent with our objectives.

The presence of a given flow field in a spatially invariant uniaxial discotic liquid crystal generates the following dynamical system :

$$\dot{\mathbf{y}} = \mathbf{Y}(\mathbf{y}(t))\,. \tag{15a}$$

$$\mathbf{y} = (\mathbf{n}, S)\,; \tag{15b}$$

$$\mathbf{y} \in \Omega^2 \times [0, 1]\,; \tag{15c}$$

$$\mathbf{y} : \mathrm{R}^+ \to \Omega^2 \times [0, 1] \tag{15d}$$

To find $\mathbf{Y}(\mathbf{y}(t))$, we use the following set of Euler-Lagrange equations [30, 31] :

$$\frac{\tilde{\delta}\Lambda}{\delta n_i} - \frac{\delta D}{\delta \dot{n}_i} = 0 \; ; \tag{16a}$$

$$\frac{\tilde{\delta}\Lambda}{\delta S} - \frac{\delta D}{\delta \dot{S}} = 0 \tag{16b}$$

$$\frac{\tilde{\delta}\Lambda}{\delta n_i} = (\delta_{ij} - n_i\, n_j)\left(\frac{\partial \Lambda}{\partial n_j} - \partial_k \frac{\partial \Lambda}{\partial(\partial_k n_j)} - \frac{\partial}{\partial t}\frac{\partial \Lambda}{\partial \dot{n}_j} \right) \tag{16c}$$

$$\frac{\tilde{\delta}\Lambda}{\delta S} = \left(\frac{\partial \Lambda}{\partial S} - \partial_k \frac{\partial \Lambda}{\partial(\partial_k S)} - \frac{\partial}{\partial t}\frac{\partial \Lambda}{\partial \dot{S}} \right) \tag{16d}$$

$$\frac{\delta D}{\delta \dot{n}_i} = (\delta_{ij} - n_i\, n_j)\left(\frac{\partial D}{\partial \dot{n}_j} - \partial_k \frac{\partial D}{\partial(\partial_k \dot{n}_j)} \right) \tag{16e}$$

$$\frac{\delta D}{\delta \dot{S}} = \frac{\partial D}{\partial \dot{S}} - \partial_k \frac{\partial D}{\partial(\partial_k \dot{S})} \tag{16f}$$

where $\tilde{\delta}\Lambda/\delta y$ is the projected total Euler-Lagrange derivative, and $\delta D/\delta \dot{y}$ is the projected space Euler-Lagrange derivative [17]. The projection operator $(\delta_{ij} - n_i\, n_j)$ that appears in the director derivatives is required to eliminate the undetermined Lagrangian multiplier that arises from the unit length constraint on the director $\mathbf{n} \cdot \mathbf{n} = 1$; for the alignment no constraints are imposed and the projector operator is unity.

As shown in the Appendix, with the choices of Λ and Δ given in the equations (7, 9, 12), the dynamics of the director $\mathbf{n}$ and the alignment S are found to be :

$$\dot{\mathbf{y}} = \begin{bmatrix} \dfrac{\mathrm{d}n_i}{\mathrm{d}t} \\ \dfrac{\mathrm{d}S}{\mathrm{d}t} \end{bmatrix} = \begin{bmatrix} W_{ij}\, n_j + \lambda\,(A_{ij}\, n_j - (A_{\ell k}\, n_\ell\, n_k)\, n_i) \\ \beta_1\, A_{\ell k}\, n_\ell\, n_k + \beta_2/\tau_1 \end{bmatrix} \tag{17a, b}$$

where $\lambda\,(S)$ is the tumbling function, $\beta_1(S)$ the ordering function, and $\beta_2(S, U)$ is proportional to $\partial \Lambda^{\mathrm{H}}/\delta S$; these functions are given by :

$$\lambda = -\frac{\gamma_2}{\gamma_1} = -\,(3\,\sigma_4^* + \sigma_6^*\, S)/(3\,S + \tau_2^*\, S^2) \tag{18a}$$

$$\beta_1 = -\,(9\,\sigma_4^* + 6\,\sigma_6^*\, S)/(6 + 4\,\tau_2^*\, S) \tag{18b}$$

$$\beta_2 = (-\,3\,S + US + US^2 - 2\,US^3)/(3 + 2\,\tau_2^*\, S) \tag{18c}$$

where the starred coefficients are scaled with the alignment relaxation time τ_1.

To select numerical values for the three phenomenological parameters σ_4^*, σ_6^*,

τ_2^*, we enforce the following constraints on the signs of λ and γ_1 [7-10] and on the values of λ when $S = 0$ and $S = 1$ [7] :

$$\lambda = -\frac{\gamma_2}{\gamma_1} < 0 ; \tag{19a}$$

$$\gamma_1 \geqslant 0 ; \tag{19b}$$

$$\lim_{S \to 0} \lambda = -\infty ; \tag{19c}$$

$$\lim_{S \to 1} \lambda = -1 . \tag{19d}$$

The adopted values that satisfy the constraints are : $\sigma_4^* = 1/10$, $\sigma_6^* = 1.7$, $\tau_2^* = -1.0$, and the resulting λ and β_1 are shown in figure 2. An indirect validation that the presently adopted values of the phenomenological coefficients, that appear in the dimensionless formulation of the governing equations for the idealized discotic nematic, may describe qualitatively some important features of the flow of real carbonaceous mesophases can be found by comparing the shear flow predictions of [32] with the experiments of [33]. In [32] the present model was solved for simple shear drag flow, using approximately similar values of the phenomenological coefficients (σ_4^*, σ_6^*, τ_2^*), and it was predicted that shear flow instabilities may set in at critical values of the shear rate ; these instabilities are transitions between flow-tumbling and flow-aligning modes that characterize nematics of variable degree of orientation and mathematically are bifurcations between two types of periodic attractors and a steady state attractor. These shear flow instabilities were previously observed experimentally in a pressure-driven shear flow of a real carbonaceous mesophase by [33], where the observed pattern formation phenomena was explained using the tumbling-aligning transition, as calculated by [32]. Lastly, other set of parameters obeying the constraints (19a, b, c, d) were used in this work, but because the present flow is irrotational and all the attractors are steady states, the only differences in the computed solution vectors will be in the time scales, and hence, for brevity, these essentially similar results are omitted here.

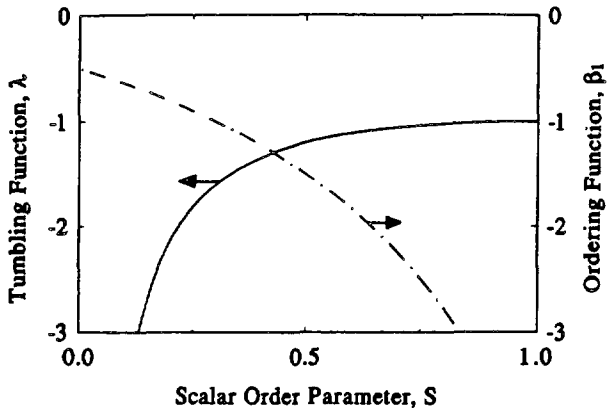

Fig. 2. — Tumbling function λ and the ordering function β_1 as a function of the scalar order parameter S. The tumbling function is the ratio of the coefficient for strain and vorticity viscous torques, while the ordering function is the coefficient for the ambient strain rate $\mathbf{A} : \mathbf{nn}$ that governs the relaxation of S. For discotics (rod-like) nematics both are negative (positive).

If the alignment S is assumed to be constant, the present model is identical to the Transversely Isotropic Fluid (TIF) model of Ericksen [34] applicable to purely viscous nematic fluids :

$$\frac{dn_i}{dt} = W_{ij}\, n_j + \lambda\,(A_{ij}\, n_j - (A_{\ell k}\, n_\ell\, n_k)\, n_i) \tag{20a}$$

$$\lambda = \text{Constant} ;$$

$$\lambda > 0 \text{ (rods)}, \quad \lambda < 0 \text{ (disks)}. \tag{20b}$$

The constant alignment case was not studied in the present paper, but rigorous results for uniaxial extensional and biaxial extensional flows for rodlike nematics using the TIF model were obtained recently [35, 36]. A direct comparison of equations (17a) and (20a) shows that for irrotational flows ($\mathbf{W} = 0$), the present model and the TIF model predict exactly the same director orbits $O(\mathbf{n}_0)$ and the only difference between the predicted director fields is the time parametrization along the orbits ; this difference is important in applications since it affects the number of strain units required to achieve a given orientation.

The following simplifying assumptions and approximations, have been made in deriving the mathematical model that describes the flow-induced alignment and orientation of an ideal discotic nematic liquid crystal, as given by equations (17, 18) : (1) the fluid is incompressible and the flow is isothermal ; (2) the orientation and alignment are space invariant ; all elastic effects due to spatial gradients are neglected ; (3) the entropy production has been arbitrarily truncated, such that it reduces to the Leslie-Ericksen expression ; (4) the three coefficients of the Landau-de Gennes excess free energy have been fitted using two parameters ; (5) fluctuations that are important near the nematic-isotropic phase transition are neglected ; (6) the velocity field is considered to be given, and therefore we dispense with solving the Cauchy equation of motion which involves the use of the nine parameters appearing in equation (7).

2.3 GOVERNING EQUATIONS FOR UNIAXIAL EXTENSIONAL START-UP FLOW. — The velocity field $\mathbf{v}(x, y, z)$ corresponding to the uniaxial extensional start-up flow of the nematic sample, is given by [26] :

$$v_x = \dot{\varepsilon} x H(t) ; \tag{21a}$$

$$v_y = -\frac{\dot{\varepsilon}}{2} y H(t) ; \tag{21b}$$

$$v_z = -\frac{\dot{\varepsilon}}{2} z H(t) ; \tag{21c}$$

$$H(t) = \begin{cases} 0 & t < 0 \\ 1 & t \geq 0 \end{cases} \tag{21d}$$

where $\dot{\varepsilon}$ is the constant extension rate. The non-zero components of the corresponding rate of deformation tensor $\mathbf{A}$ are : $A_{11} = \dot{\varepsilon}$; $A_{22} = A_{33} = -\dot{\varepsilon}/2$; this flow is irrotational and the vorticity tensor $\mathbf{W} = \mathbf{0}$. A useful decomposition of the director field $\mathbf{n}$ and the rate of deformation tensor $\mathbf{A}$ is :

$$\mathbf{n} = \mathbf{n}_\perp + \mathbf{n}_\parallel ; \tag{22a}$$

$$\mathbf{n}_\perp = n_y \hat{\mathbf{j}} + n_z \hat{\mathbf{k}} ; \tag{22b}$$

$$\mathbf{n}_\parallel = n_x \hat{\mathbf{i}} ; \tag{22c}$$

$$\mathbf{A} = \dot{\varepsilon}\delta - \frac{3}{2}\dot{\varepsilon}\mathbf{P} \tag{22d}$$

where $\delta = \hat{\mathbf{i}}\hat{\mathbf{i}} + \hat{\mathbf{j}}\hat{\mathbf{j}} + \hat{\mathbf{k}}\hat{\mathbf{k}}$ and $\mathbf{P} = \hat{\mathbf{j}}\hat{\mathbf{j}} + \hat{\mathbf{k}}\hat{\mathbf{k}}$. Replacing equations (21, 22) into equations (17a, 17b), we obtain the following dimensionless set of coupled nonlinear ordinary differential equations :

$$\begin{bmatrix} \dfrac{d\mathbf{n}_\perp}{d\varepsilon} \\ \dfrac{dS}{d\varepsilon} \end{bmatrix} = \begin{bmatrix} \dfrac{3}{2}\lambda\,(n_\perp^2 - 1)\,\mathbf{n}_\perp \\ \dfrac{\beta_1}{2}\,(2 - 3\,n_\perp^2) + \mathrm{De}^{-1}\,\beta_2 \end{bmatrix} \tag{23a, b}$$

$$n_\shortparallel = \text{sign}\,(n_\shortparallel\,(t = 0))\,\sqrt{1 - n_\perp^2} \tag{23c}$$

where $\varepsilon = \dot{\varepsilon} t$ is the strain, $\mathrm{De} = \dot{\varepsilon}\tau_1$ is the alignment Deborah number (dimensionless strain rate). When $\mathrm{De} \to 0$ the alignment (S) relaxation is elastic, when $\mathrm{De} \to \infty$ it is purely viscous, and for the intermediate values it is viscoelastic. At intermediate De the director relaxation is also viscoelastic, since it is coupled to S through $\lambda\,(S)$.

The initial conditions used to solve equations (23) are : @$\varepsilon = 0$: $\mathbf{n} = \mathbf{n}_0$; $S_0 = S_{eq}$, $\mathbf{n}_0 \cdot \mathbf{n}_0 = 1$, where $S_0 = S_{eq}(U)$ is given by equation (14b). In this paper we use two representative nematic potentials $U = 3$ and $U = 5$, and the corresponding initial conditions are : $S_{eq}(U = 3) = 0.5$ and $S_{eq}(U = 5) = 0.76$. All angles are reported in degrees.

Equations (23a, 23b) are integrated using an implicit corrector-predictor first order Euler integration method with an adaptable time step [37]. Application of the implicit corrector-predictor method transforms the set of coupled nonlinear ordinary differential equations (23a, 23b) into a set of coupled nonlinear algebraic equations. For each time step the algebraic equations are solved using the Newton-Raphson iteration scheme [37] ; the predictor step generates a first guess for the iteration loop and the corrector step is the iteration loop itself. The adopted convergence criteria is that the length of the difference vector between the calculated solution vectors corresponding to two successive iterations is less than 10^{-6} The transient solution vector obtained from the numerical solutions ($\mathbf{n}(\varepsilon)$, $S(\varepsilon)$), is used to calculate the tensor order parameter $\mathbf{Q}(\varepsilon)$. and the converged steady state solutions ($\mathbf{n}_{ss}$, S_{ss}) are used to compute the steady flow birefringence. To facilitate the discussion and perform an analysis of the numerical solutions, some of the computed results are presented in reference to the unit sphere description of the director field.

3. Results and discussions.

3.1 DIRECTOR DYNAMICS · GEODESIC FLOW AND VISCOELASTIC RELAXATION. — Integration of equation (17) yields, for $\mathbf{W} = 0$ and for $\mathbf{A}$ as defined above, the following expression for the director relaxation $\mathbf{n}(\varepsilon)$ for the uniaxial extension start-up flow :

$$n_i(\varepsilon) = \frac{E_{ij}\,n_{j0}}{|\mathbf{E} \cdot \mathbf{n}_0|} ;$$

$$n_i(0) = n_{i0} ;$$

$$E_{ij}(\varepsilon) = \exp\left\{\tilde{A}_{ij} \int_0^\varepsilon \lambda\, d\varepsilon'\right\} ;$$

$$\tilde{A}_{ij} = A_{ij}/\dot{\varepsilon} \tag{24}$$

and in the component form :

$$n_1 = \frac{E_{11}\, n_{10}}{|\mathbf{E}\cdot\mathbf{n}_0|}, \quad n_2 = \frac{E_{22}\, n_{20}}{|\mathbf{E}\cdot\mathbf{n}_0|}; \quad n_3 = \frac{E_{33}\, n_{30}}{|\mathbf{E}\cdot\mathbf{n}_0|} \tag{25a}$$

$$E_{11} = \exp\left(\int_0^t \lambda\, d\varepsilon'\right); \quad E_{22} = E_{33} = \exp\left(-\frac{1}{2}\int_0^t \lambda\, d\varepsilon'\right); \quad E_{ij} = 0 \quad \text{for} \quad i \neq j \tag{25b}$$

where n_{j0} is the jth component of the initial director orientation ($\mathbf{n}(0)$). From (25a, 25b) it follows that $n_2 = bn_3$ ($b = n_{20}/n_{30}$), and comparing with equations (5, 6) it follows that the

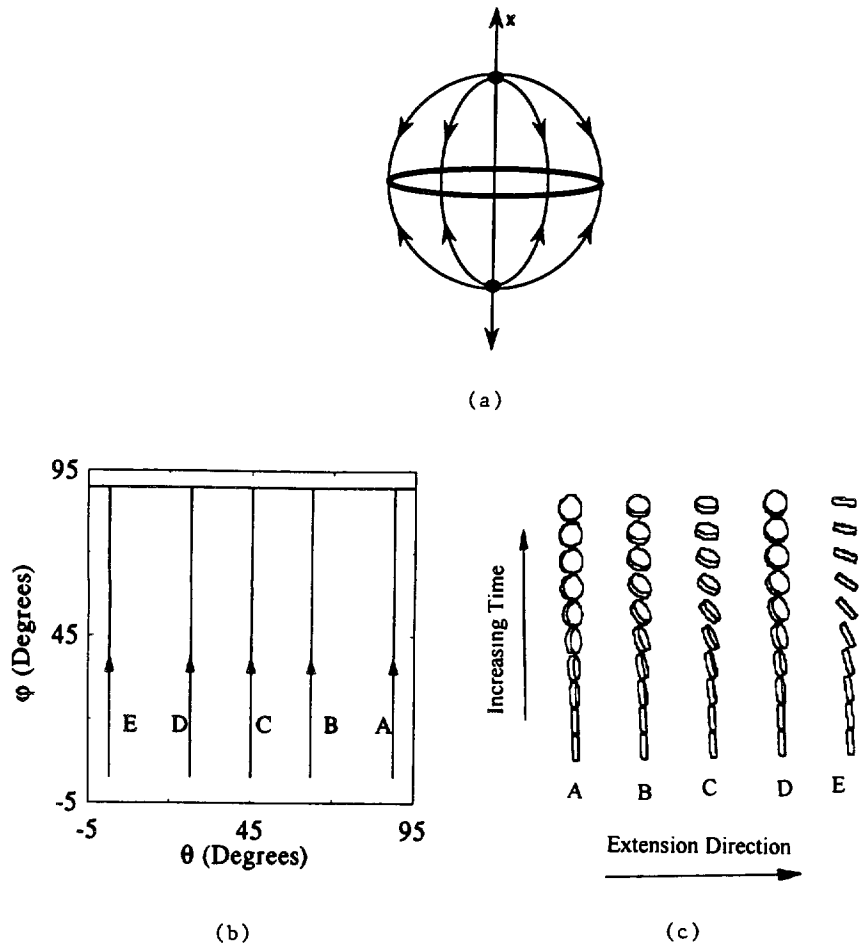

Fig. 3. — Sensitivity of the director orbits to the initial conditions. (a) Schematic of the unit sphere and several meridians (great circles through the poles) ; the x-direction is along the extension direction and the equator represents the degenerate circle of stable steady director orientations. (b) Polar angle ϕ as a function of the azimuthal angle θ for $U = 5$ and De = 1, and for the following director initial orientations (θ_0, ϕ_0): $A = (88.72,\ 2.56)$, $B = (63.4,\ 2.56)$, $C = (45,\ 2.56)$, $D = (26.56,\ 2.56)$, $E = (1.28,\ 2.56)$. (c) Corresponding computed scientific visualization of the director relaxation, represented by the normals to the shown discs. Predictability is lost when the initial orientation is on the poles ; close to the poles there is high sensitivity to $\mathbf{n}_0$.

director orbits belong to the meridians, and the director dynamics belong to the class of geodesic flows. Therefore the present problem should exhibits the characteristic sensitive dependence on initial conditions, that is typical of geodesic flows [38]. Equations (25a, 25b) shows that the stable director steady states are $\mathbf{n}_{\infty} = (0, n_{\backslash 0}/n_{\perp 0}, n_{/0}/n_{\perp 0})$.

The director orbit follows a geodesic flow due to the inherent symmetry in the uniaxial extensional flow. This result is also predicted by the TIF equation (20a), since as mentioned above, for irrotational flows the geometry of the director orbits are insensitive to variations in the magnitude of the alignment.

Figure 3a shows that the unit sphere with representative meridians, figure 3b shows the computed polar angle ϕ as a function of azimuthal angle θ, and figure 3c shows the corresponding computed scientific visualization of the average disc's relaxation, for $U = 5$ and $De = 1$, and the following director initial orientations (θ_0, ϕ_0): $A = (88.72, 2.56)$, $B = (63.4, 2.56)$, $C = (45, 2.56)$, $D = (26.56, 2.56)$, $E = (1.28, 2.56)$. Figure 3a shows that when starting on the poles, the director steady states, depicted by the equator, are unpredictable. The (θ, ϕ) plot shows that the final steady state, denoted by the upper horizontal line, is highly sensitive to small variations of the initial orientation when the initial director tip is next to the poles. The computed director orbits follow the meridians defined by equations (5, 6). The visualizations shows the director (normal to the shown discs)

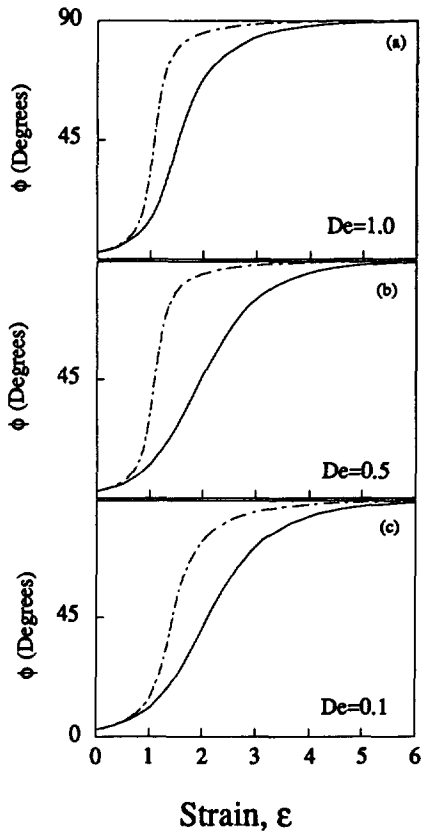

Fig. 4. — Polar director angle ϕ as a function of strain ε, for De = 1 (a), 0.5 (b), and 0.1 (c); $U = 3$ (dash-dot line), $U = 5$ (solid line), and the initial director orientation $(\theta_0, \phi_0) = (45, 2.56)$. The director relaxation is viscoelastic, and it is faster at higher De and at lower U.

relaxation, along the five different paths, exhibiting different combinations of tilting and twisting along the time axis, but eventually leading to a stable orientation on the plane $(y - z)$, normal to the extensional direction.

Figure 4 shows the polar director angle ϕ as a function of strain ε, for De = 1 (a), 0.5 (b), and 0.1 (c) ; $U = 3$ (dash-dot line), $U = 5$ (solid line), and $(\theta_0, \phi_0) = (45, 2.56)$. The figure shows that the director relaxation is viscoelastic, and that it is faster at higher De and at lower U, since for these conditions λ samples larger absolute values.

3.2 ALIGNMENT VISCOELASTIC RELAXATION AND FLOW INDUCED MELTING. — The alignment $S(\varepsilon)$ relaxation depends on $\mathbf{n}_0$ through the ambient strain rate **A : nn**. Figure 5a shows the three representative regions for **A : nn** in the two equivalent spherical caps R_1 the rate is positive

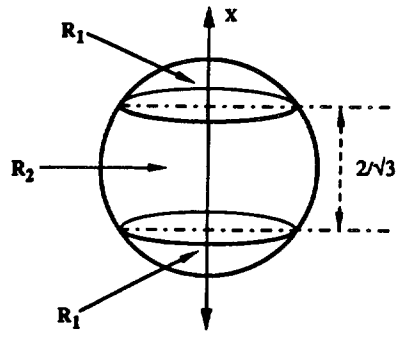

(a)

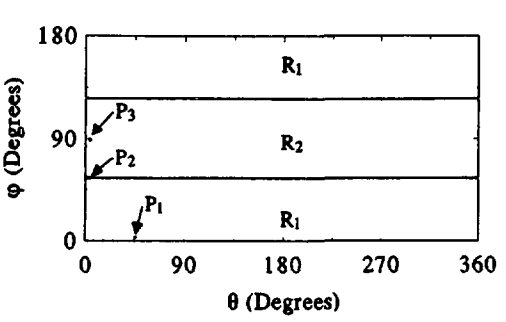

(b)

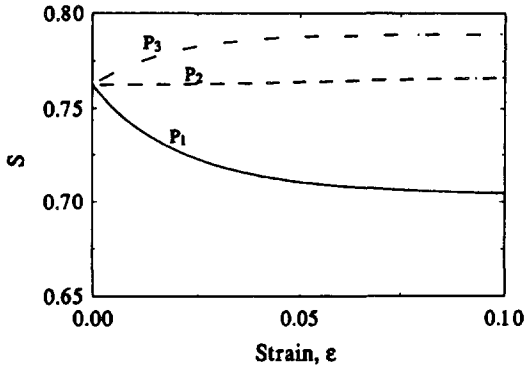

(c)

Fig. 5. — Sensitivity of the initial alignment S relaxation to the initial director orientation. (a) The three characteristic regions for the ambient strain rate **A : nn**. (b) Planar (θ, ϕ) representation of the three representative regions for **A : nn** : where **A : nn** > 0 on the two equivalent upper and lower rectangles (R_1) and **A : nn** < 0 on the middle rectangle (R_2) to the two closed curves, and three characteristic initial orientations (θ_0, ϕ_0) : $P_1 = (45, 2.56)$ in R_1, $P_2 = (0.9, 54.7)$ in $\partial R_1 = \partial R_2$, and $P_3 = (2.56, 89.9)$ in R_2. (c) Initial alignment S relaxation for De = 0.1 and $U = 5$.

$(\mathbf{A} : \mathbf{nn} > 0)$, and in the spherical zone R_2 the rate is negative $(\mathbf{A} : \mathbf{nn} < 0)$. The initial alignment relaxation characteristics are given by :

$$\mathbf{n}_0 \quad \text{in} \quad R_1 \,.\, \left(\frac{dS}{d\varepsilon} \right)_{\varepsilon = 0^+} < 0 \,; \tag{26a}$$

$$\mathbf{n}_0 \quad \text{in} \quad R_2 \,.\, \left(\frac{dS}{d\varepsilon} \right)_{\varepsilon = 0^+} > 0 \,; \tag{26b}$$

$$\mathbf{n}_0 \quad \text{in} \quad \partial R_1 = \partial R_2 \,.\, \left(\frac{dS}{d\varepsilon} \right)_{\varepsilon = 0^+} = 0 \,. \tag{26c}$$

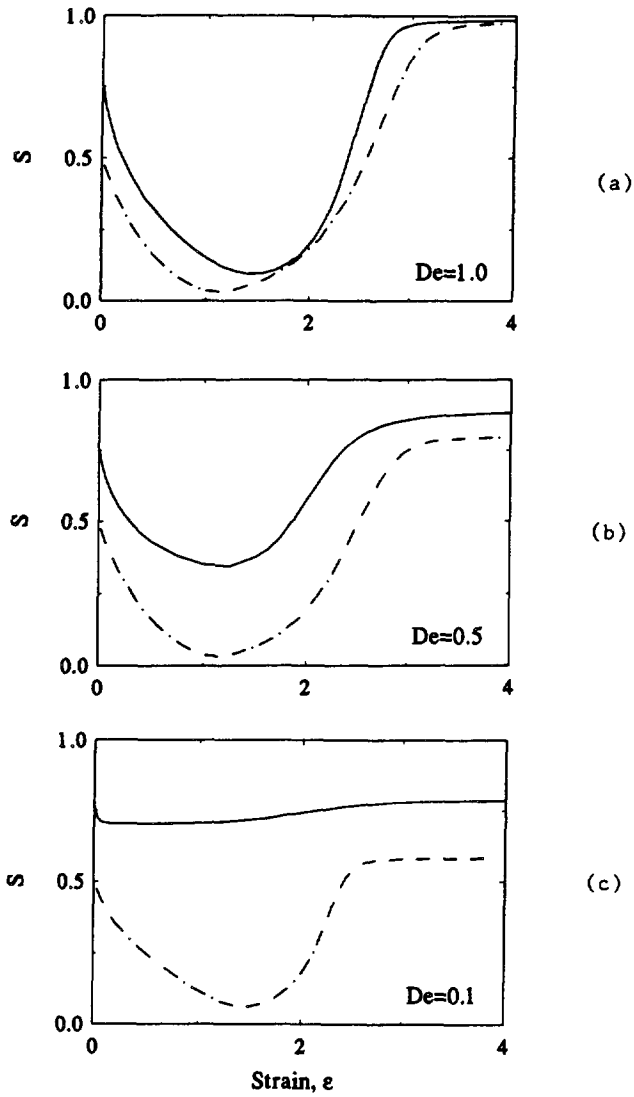

Fig. 6. — Alignment relaxation $S(\varepsilon)$, corresponding to the conditions of the director relaxation of figure 4. The figure shows that at higher De the viscous mode dominates and the effect of relative magnitude of U is small, while at lower De the elastic mode dominates and the effect of relative magnitude of U is large.

Figure 5b shows the three representative regions for **A** : **nn**, where the upper and lower rectangles represent R_1, and the middle rectangle represents R_2, and three characteristic initial orientations (θ_0, ϕ_0): $P_1 = (45, 2.56)$ in R_1, $P_2 = (0.9, 54.7)$ in $\partial R_1 = \partial R_2$, and $P_3 = (2.56, 89.9)$ in R_2. Figure 5c shows the corresponding initial alignment S relaxation for De = 0.1 and $U = 5$. It follows that for any De, a sufficient condition for increasing S is that **n** is in R_2.

Figure 6 shows the alignment relaxation $S(\varepsilon)$, corresponding to the conditions of the director relaxation of figure 4. The figure shows that at higher De (De = 1), the viscous mode dominates the viscoelastic relaxation at all the times, and the effect of the relative magnitude of U is small. At lower De (De = 0.1), the elastic mode dominates at all times if $U = 5$, and negligible changes occur since $S_0 \approx S_{eq}$, while for $U = 3$ the viscous mode dominates the initial response, but the elastic mode dominates the later stage. Since in this figure $\mathbf{n}_0$ is in R_1, the alignment relaxation always shows an initial decrease in S. Comparing the steady state alignment S_{ss} for all cases, it is seen that at larger De, the viscous mode dominates and the effect of U is small, while at lower De, the elastic mode dominates and the effect of U is large.

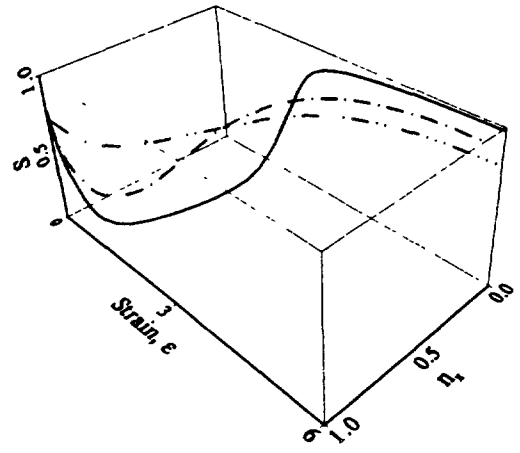

(a)

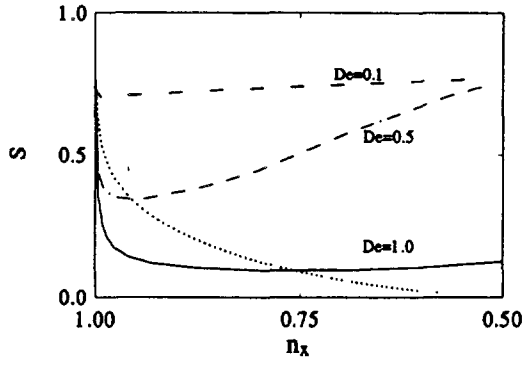

(b)

Fig. 7. — (a) Alignment S and x-component of the director n_x as a function of strain ε, and (b) projection of figure 7a on the (S, n_x) plane, with the initial orientation $(\theta_0, \phi_0) = (45, 2.56)$ close to the pole, for $U = 5$, and De = 0.1 (dash-triple dot line), 0.5 (dash-dot line), and 1 (full line). The dotted line corresponds to $dS/dn_x = 0$; at high De discotic nematics undergo practically a temporary melting while the director is in $R_1 (n_x > (3)^{-1/2})$.

Figure 7a shows the alignment S and x-component of the director n_x as a function of strain ε, and figure 7b shows the projection of figure 7a on the (S, n_x) plane, with the initial orientation $(\theta_0, \phi_0) = (45, 2.56)$ close to the pole, for $U = 5$, and De = 0.1 (dash-triple dot line), 0.5 (dash-dot line), and 1 (full line). Figure 7a shows the coupling of the orientation and alignment relaxations, which indicates that by increasing De the increasing relaxation follows a two step process : an initial decrease in S followed by monotonic increase (decrease) in $S(n_x)$. The nature of the (n_x, S) coupling is shown in figure 7b, where the dotted line corresponds to $dS/dn_x = 0$. For the given $\mathbf{n}_0$, the higher De the lower the value of n_x at which S starts increasing ; for large De, discotic nematics undergo practically a temporary melting while the director is in R_1 $(n_x > (3)^{-1/2})$. For this particular case a more accurate model should include the fluctuations that are present near the isotropic-nematic phase transition.

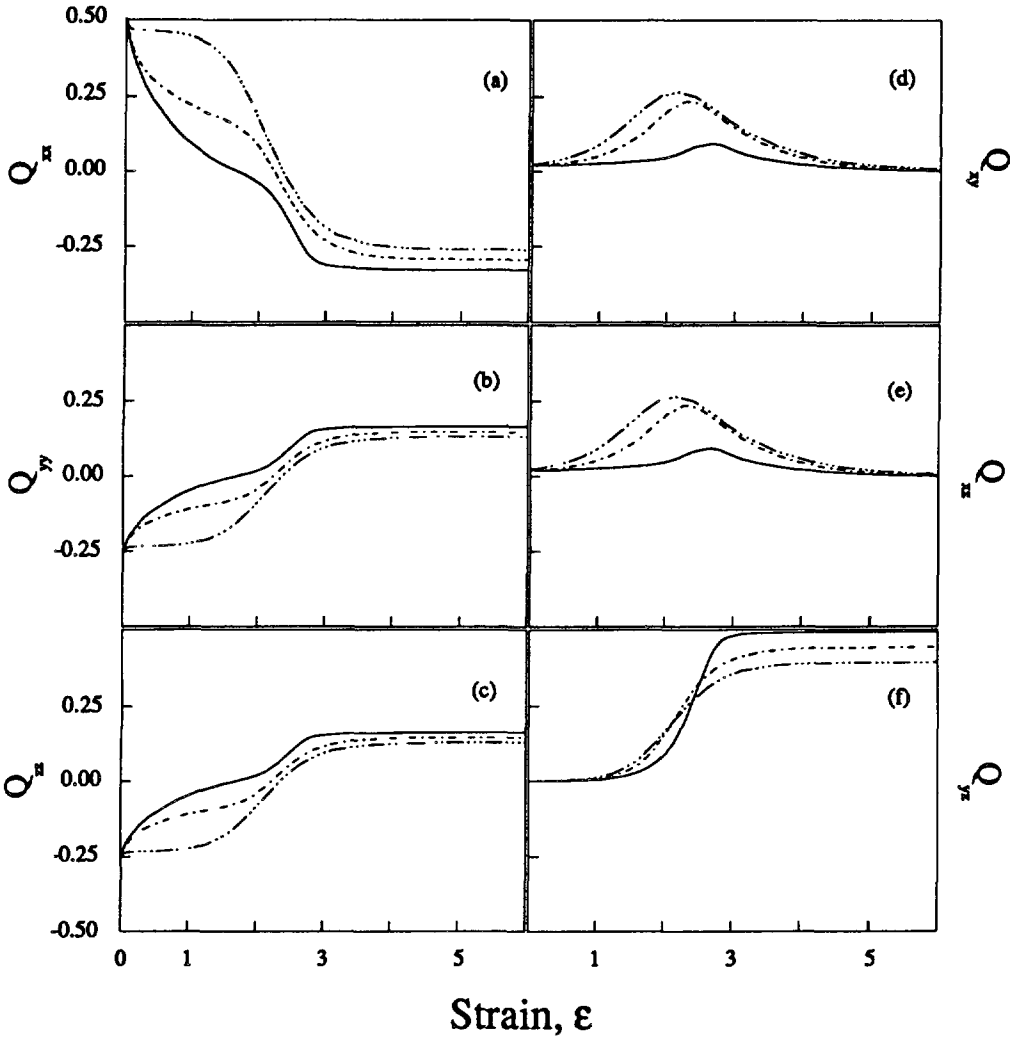

Fig. 8. — Relaxation of the components of the tensor order parameter **Q** with the initial orientation $(\theta_0, \phi_0) = (45, 2.56)$ close to the pole, for $U = 5$, and De = 0.1 (triple dot-dash line), 0.5 (dash-dot line), and 1 (full line). For the chosen initial orientation $n_{y0} = n_{z0}$, and from equation (6) it follows that $Q_{xx} = Q_{yz}$ and $Q_{zz} = Q_{yy}$.

In contrast to the steady state director orientation which may exhibit a strong sensitivity to the initial orientation, the steady state scalar order parameter is independent of the initial orientation, and depends on the magnitudes of De and U, as shown by the lower equation (23b).

3.3 TENSOR ORDER PARAMETER RELAXATION AND FLOW BIREFRINGENCE. — Figure 8 shows the relaxation of the components of the tensor order parameter **Q** with the initial orientation $(\theta_0, \phi_0) = (45, 2.56)$ close to the pole, for $U = 5$, and De = 0.1 (triple dot-dash line), 0.5 (dash-dot line), and 1 (full line). For the chosen initial orientation $n_{y0} = n_{z0}$, and from equation (6) it follows that $Q_{xy} = Q_{xz}$ and $Q_{zz} = Q_{yy}$. For the shown parameters the relaxation is virtually complete after 5 strain units. At low De the relaxation of the trace components (Q_{ii}) are dominated by the director relaxation shown in figure 4, since for $U = 5$ the alignment is nearly constant (see Fig. 6). At higher De the relaxation of the trace components is dominated by the viscous mode, and reflects the two step process described in figure 7. At low De the non-diagonal terms of **Q** are again governed by the director relaxation, while at higher De, the viscous effect introduces an initial large decrease in S while **n** is in R_1 and a subsequent increase in S while **n** is in R_2, with the result that the only large component is Q_{yz}, which follows a lag plus exponential growth relaxation.

According to [27], the birefringence $\Delta\eta$ can be expressed by :

$$\Delta\eta = \sqrt{e_{\parallel}} - \sqrt{e_{\perp}} \approx \frac{\Delta e_{\max} S}{2\sqrt{\tilde{e}}} \tag{27}$$

where $e_{\parallel}$ and $e_{\perp}$ are the elements of the dielectric tensor e_{ij} parallel and normal to the director, the tensor is given by $e_{ij} = \tilde{e}\delta_{ij} + \Delta e_{\max} Q_{ij}$, where the first term is the average trace of e_{ij} and $\Delta e_{\max}$ is the anisotropy for $S = 1$; for discotics, $\Delta\eta < 0$ since $\Delta e_{\max} < 0$. In deriving equation (27) we have assumed that $\tilde{e} \gg 2\,\Delta e_{\max} S/3$ for the values of S corresponding to the nematic phase. Equation (27) shows that the steady flow-induced birefringence $\Delta\eta_{ss}$ is proportional to the magnitude of the steady alignment S_{xy}.

Figure 9 shows the steady state alignment S_{ss} as a function of De, for $U = 3$ (dash-dot line) and $U = 5$ (full line). The figure shows a monotonic increase in the flow birefringence, at high De the viscous mode dominates and the effect of the magnitude of U is small, while at low De the elastic mode dominates and the effect of the magnitude of U on S_{ss} is large.

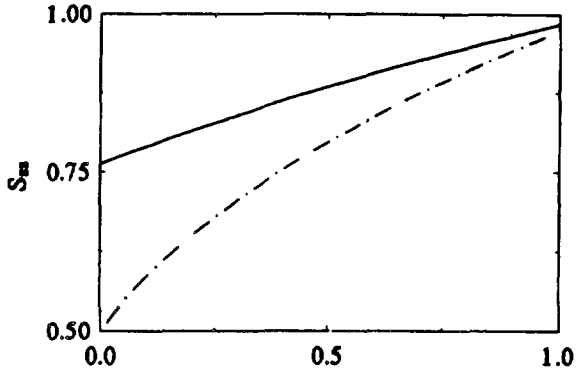

Fig. 9. — Steady state alignment S_{xy} as a function of De, for $U = 3$ (dash-dot line) and $U = 5$ (full line). The flow birefringence is proportional to S_{xy} and increases with De.

4. Conclusions.

In this initial investigation of the nematorheology of uniaxial discotics in uniaxial extensional flows, we have performed a useful characterization of the sensitivity of the director, scalar order parameter, and tensor order parameter relaxation with respect to the nematic potential, the alignment Deborah number, and the initial director orientation. Use of unit sphere description identified the director dynamics as a geodesic flow. This observation is used to explain the loss of predictability when the director is initially aligned along the extension direction, and allows for the use of the simple geometrical principle to identify the director orbits. The identification of the governing De parameter allows for the classification into the different elastic and viscous dominated relaxations. For large De, temporarily flow induced melting of the nematic phase may occur. This unified picture of relaxation under extension may be used to explain the characteristic patterns found in the cross-section of melt spun carbonaceous mesophases. In the extension-dominated flow process the normals to the molecular planes always align anywhere in the plane normal to the fiber axis, as shown in this paper for the stretching of a model discotic. The present analysis provides for a basis for the more general spatially in homogeneous case, where Frank elasticity must be included.

Acknowledgments.

This work is supported by a grant from the Natural Sciences and Engineering Research Council of Canada.

Appendix.

Substituting of equations (1) into (7), and the negative of equation (13) yield, respectively, the following equations for the dissipation Δ and the Langrangian A^{H} :

$$2\,D(\nu KT)^{-1} = \Delta(\nu KT)^{-1} = \alpha_1(n_i\,A_{ik}\,n_k)^2 + \alpha_4\,A_{ij}\,A_{ji} + (\alpha_5+\alpha_6)(n_j\,A_{jk}\,A_{k\ell}\,n_\ell) + \\ + \gamma_1 N_i^2 + 2\,\gamma_2\,n_i\,A_{ij}\,N_j + \mu_1\,\dot{S}^2 + \mu_2\,\dot{S}(n_i\,A_{ij}\,n_j) \quad \text{(A.1)}$$

$$A^{H} = -\,\nu KT\left\{\frac{1}{9}(3-U)\,S^2 - \frac{2}{27}\,US^3 + \frac{1}{9}\,US^4\right\} \quad \text{(A.2)}$$

where :

$$\alpha_1 = \sigma_1\,S^2 \quad \text{(A.3a)}$$

$$\alpha_4 = \sigma_2 - 2\,\sigma_5\,S/3 + 2(\sigma_3 + \sigma_7/3)\,S^2/3 \quad \text{(A.3b)}$$

$$\alpha_5 + \alpha_6 = 2\,\sigma_5\,S + 2\,\sigma_7\,S^2/3 \quad \text{(A.3c)}$$

$$\gamma_1 = 2(\tau_1 + \tau_2\,S/3)\,S^2 \quad \text{(A.3d)}$$

$$\gamma_2 = 2(\sigma_4 + \sigma_6\,S/3)\,S \quad \text{(A.3e)}$$

$$\mu_1 = 2(3\,\tau_1 + 2\,\tau_2\,S)/9 \quad \text{(A.3f)}$$

$$\mu_2 = 2(9\,\sigma_4 + 6\,\sigma_6\,S)/9 \quad \text{(A.3g)}$$

$$N_i = \frac{\partial n_i}{\partial t} + (v_j\,\partial_j)\,n_i - W_{ij}\,n_j\,. \quad \text{(A.3h)}$$

Taking the space Euler-Lagrange derivative of D (Eqs. (16e, 16f)), yields :

$$\frac{\tilde{\delta} D}{\partial \dot{n}_i} = \nu KT(\delta_{ij} - n_i n_j)(\gamma_1 N_j + \gamma_2 A_{j\ell} n_\ell + \chi n_j) \tag{A.4a}$$

$$\frac{\tilde{\delta} D}{\partial \dot{S}} = \nu KT(\mu_1 S + \mu_2 A_{j\ell} n_j n_\ell/2) \tag{A.4b}$$

where χ is a scalar Lagrange multiplier. Taking the total Euler-Lagrange derivative of A^H (Eqs. (16c, 16d)) yields :

$$\frac{\delta A^H}{\delta n_i} = 0 \tag{A.5a}$$

$$\frac{\delta A^H}{\partial S} = -\nu KT[2[(3 - U)S - US^2 + 2US^3]/9]. \tag{A.5b}$$

Subtracting equation (A.4a) from equation (A.5a), and equation (A.4b) from equation (A.5b) yields :

$$(\delta_{ij} - n_i n_j)(\gamma_1 N_j + \gamma_2 A_{jk} n_k + \chi n_j) = 0 \tag{A.6}$$

$$-2[(3 - U)S - US^2 + 2US^3]/9 - \mu_1 \dot{S} - \frac{1}{2}\mu_2 A_{\ell k} n_k n_\ell = 0 \tag{A.7}$$

which yield equations (17a, 17b), upon the following identification

$$\lambda = -\frac{\gamma_2}{\gamma_1} \qquad \beta_1 = -\frac{\mu_2}{2\mu_1} \qquad \frac{\beta_2}{\tau_1} = -\frac{2[(3 - U)S - US^2 + 2US^3]/9}{\mu_1} \tag{A.8}$$

References

[1] Gasparoux H., *Mol. Cryst Liq Cryst.* **63** (1981) 231-248.

[2] Otani S., *Mol. Cryst Liq. Cryst.* **63** (1981) 249-264.

[3] Zimmer J. E., White J. L., Disclination Structures in the Carbonaceous Mesophase. H. G. Brown Ed., Advances in liquid Crystals, Vol. **5** (Academic Press, New York, 1982).

[4] Chandrashekhar S., *Mol Cryst. Liq. Cryst.* **63** (1981) 171-179.

[5] Destrade C., Tinh N. H., Gasparoux H., Malthete J., Levelut A. M., *Mol. Cryst. Liq. Cryst.* **71** (1981) 111-135.

[6] Singer L. S., The Mesophase in Carbonaceous Pitches, *Faraday Discuss Chem. Soc.* **73** (1985) 265-272.

[7] Volovik G. E., *JETP Lett* **31** (1980) 273-275.

[8] Carlsson T., *Mol. Cryst. Liq Cryst* **89** (1982) 57-66.

[9] Carlsson T., *J. Phys. France* **44** (1983) 909-911.

[10] Baals H., Hess S., *Z. Naturforsch.* **43 A** (1988) 662-670.

[11] Ho A. S. K., Rey A. D., *Rheol Acta* **30** (1991) 77-88.

[12] Leslie F. M., Theory of Flow Phenomena in Liquid Crystals, H. G. Brown Ed., Advances in Liquid Crystals vol. **4** (Academic Press, New York, 1981, pp. 1-81.

[13] de Gennes P. G., The Physics of Liquid Crystals (Oxford University Press, London, 1975, pp. 153-165.

[14] Ericksen J. L., Liquid Crystals with variable degree of Orientation, IMA Preprint Series No. **559** (1989).

[15] Imura H., Okano K., *Jpn J. Appl Phys* **11** (1972) 1440-1445.
[16] Diogo A. C., Martins A. F., *J. Phys. France* **43** (1982) 779-786.
[17] Edwards B. J., Beris A. N., Grmela M., *Mol. Cryst Liq Cryst.* **201** (1991) 51-86.
[18] Farhoudi Y., Rey A. D., *J. Rheol.* **37** (1993) 289-314.
[19] Marrucci G., Rheology of Nematic Polymers, A. Ciferri Ed., Liquid Crystallinity in Polymers (VCH Publishers, New York, 1991) pp. 395-423.
[20] Larson R. G., Macromolecules **23** (1990) 3893-3992.
[21] Honda, *Mol. Cryst Liq. Cryst* **94** (1983) 97-108.
[22] Thurston R. N., *J Phys. France* **42** (1981) 413-417.
[23] Thurston R. N., *J Appl. Phys.* **52** (1981) 3040-3052.
[24] Porte G., Jadot J. P., *J. Phys. France* **39** (1978) 213-223.
[25] Carlsson T., *Phys. Rev. A* **34** (1986) 3393-3404.
[26] Bird R., Armstrong R. C., Hassager O., Dynamics of Polymeric Liquids (Wiley, New York, 1987).
[27] Gramsbergen E. F., Longa L., de Jeu W. H., *Phys Rep.* **135** (1986) 195-257.
[28] Weinstock R., Calculus of Variations (McGraw-Hill, New York, 1954) pp. 26-28.
[29] Doi M., Edwards S. F., The Theory of Polymer Dynamics (Oxford University Press, New York, 1986) pp. 358-362.
[30] Hurd A. J., Fraden S., Lonberg F., Meyer R. B., *J Phys. France* **46** (1985) 905-917.
[31] Maugin G. A., *J. Non-Equilib. Thermodyn.* **15** (1990) 173-192.
[32] Farhoudi Y., Rey A. D., *Rheol. Acta* **32** (1993) 207-217.
[33] Fathollahi B., Gopalakrishnan M. K., White J. L., Carbon 92, *Proth. 5th Intl. Conf.* **A** 5 (1992) 36-38.
[34] Ericksen J. L., *Koll Zeit* **173** (1960) 117-122.
[35] Duffy B. R., *J. Non. Fluid Mech.* **28** (1988) 77-97.
[36] MacMillan E. H., *J. Rheol.* **33** (1989) 1071-1105.
[37] Finlayson B. A., Nonlinear Analysis in Chemical Engineering (McGraw-Hill, New York, 1980) pp. 28-31.
[38] Ruelle D., Chance and Chaos (Princeton University Press, New Jersey, 1991) p. 47.